Development and characterization of a novel, antimicrobial, sterile hydrogel dressing for burn wounds: Single step production with gamma irradiation creates silver nanoparticles and radical polymerization

Benjawan Boonkaew [1,*], Philip M. Barber [2], Sirirat Rengpipat [3], Pitt Supaphol [4], Margit Kempf [5], Jibao He [6], Vijay T. John [1], Leila Cuttle [5, 7]

[1] Department of Chemical and Biomolecular Engineering, Tulane University, New Orleans, Louisiana 70118, United states

[2] School of Medicine, The University of Queensland, Herston, Brisbane, Queensland 4006, Australia

[3] Department of Microbiology, Faculty of Science, Chulalongkorn University, Pathumwan, Bangkok, 10330, Thailand

[4] The Petroleum and Petrochemical College, Chulalongkorn University, Pathumwan, Bangkok 10330, Thailand

[5] Centre for Children's Burns and Trauma Research, Queensland Children's Medical Research Institute, The University of Queensland, Herston, Brisbane, Queensland 4029, Australia

[6] Coordinated Instrument Facility, Department of Physics and Engineering Physics, Tulane University, New Orleans, Louisiana 70118, United States

[7] Tissue Repair and Regeneration Program, Institute of Health and Biomedical Innovation, Queensland University of Technology, Kelvin Grove, Brisbane, Queensland 4059, Australia

Corresponding author at: Department of Chemical and Biomolecular Engineering, Tulane University, 6823 St. Charles Avenue, New Orleans, Louisiana 70118, United states. Phone: (+1504) 314-7668; E-mail address: bboonkae@tulane.edu (B. Boonkaew)

ABSTRACT

Patients with burn wounds are susceptible to wound infection and sepsis. This research introduces a novel burn wound dressing which contains silver nanoparticles (SNP) to treat infection in a 2-acrylamido-2-methylpropane sulfonic acid sodium salt (AMPS-Na^+) hydrogel. Silver nitrate was dissolved in AMPS-Na^+ solution and then exposed to gamma irradiation to form SNP infused hydrogels. The gamma irradiation results in a crosslinked polymeric network of sterile hydrogel dressing and a reduction of silver ions to form SNP

infused in the hydrogel in a one step process. About 80% of the total silver was released from the hydrogels after 72 h immersion in simulated body fluid (SBF) solution, therefore; they are suggested to be use on wounds for 3 days. All the hydrogels were found to be non-toxic to normal human dermal fibroblast (NHDF) cells. The silver loaded hydrogels had good inhibitory action against *Pseudomonas aeruginosa* and methicillin-resistant *Staphylococcus aureus* (MRSA). Results from a pilot study on a porcine burn model showed that the 5 mM silver hydrogel was efficient at preventing wounds from bacterial colonization and the results were comparable to the commercially available silver dressings (Acticoat™, PolyMem Silver®). These results support its use as a potential burn wound dressing.

KEYWORDS: hydrogels; dressings; burn wounds; antimicrobial activity; cell culture; nanoparticles; silver; gamma irradiation; spectroscopy; polymer synthesis

INTRODUCTION

The antimicrobial properties of silver have been known for many centuries and silver has a long history of use as a clinical antimicrobial agent. In 1884, silver nitrate solution was commonly used to eliminate blindness caused by postpartum infections in newborns [1]. In 1964, 0.5% silver nitrate solution was first introduced to burn care and this attracted a research interest in silver for several years afterwards [2]. The breakthrough discovery of silver sulfadiazine cream for treatment of burn wound infections in the late 1960s [3, 4] has prompted the use of silver in topical antimicrobial agents over the last four decades. In 1993, the antibacterial efficacy of various metals was noted and silver was found to have the most effective antibacterial action with the least toxicity to animal cells [5].

Once antibiotics were discovered, the use of silver as a bacterial agent decreased. However, with the increasing prevalence of antibiotic-resistant strains such as methicillin-resistant *Staphylococcus aureus* (MRSA) and Vancomycin-resistant enterococci (VRE), there has recently been a renewed interest in using silver as an antibacterial agent for burn wounds, particularly as microbial resistance to silver is rare [6]. Although the antimicrobial properties of silver ions have been known for hundreds of years, the mechanisms behind its inhibition of bacterial growth have only recently been elucidated. Silver ions may deactivate bacterial key enzymes [7] or enter the cell and intercalate between the purine and pyrimidine base pairs of DNA, disrupting the bond between the two strands and leading to DNA denaturation [4, 8]

The advent of nanotechnology resulted in the development of nanocrystalline silver containing dressings for burn wound treatment [9, 10]. Nanocrystalline silver dressings are widely used and are well known antimicrobial treatments for burns and chronic wounds [11]. Silver nanoparticles (SNP) have been infused into wound dressings, and *in vitro* studies have found them to inhibit *Pseudomonas aeruginosa* and *Staphylococcus aureus* [12]. Recently, antimicrobial gels containing SNP were found to have low toxicity and effective inhibition of *Staphylococus sp*. and *Pseudomonas aeruginosa* cell growth [13]. The advantage of smaller particles is that their surface area to volume ratio increases and more reactions can take place in a short time between molecules on the surface [14]. SNP show efficient antimicrobial activity compared to silver salts because of their larger surface area, which provides greater contact with microbes. [15]. In addition, SNP are more effective than silver ions as silver ions form salts with halides resulting in an inert silver form [6] causing a short lived antimicrobial effect. In contrast, SNP allow a steady release of silver resulting in a long-term antimicrobial activity [16].

In general, the antimicrobial mechanism of SNP is similar to that of silver ions [17]. There are several possible mechanisms for the antimicrobial mechanisms of SNP: SNP may adhere to the microbial cells, interrupting transmembrane electron transfer; They may penetrate inside bacterial cells, oxidizing cell components, or; SNP may dissolve into silver ions which can also react with proteins and DNA, adding their effects to the action of SNP [17, 18].

The selection of a suitable dressing for each wound is an important step in the treatment process. Hydrogels are popular dressings because of their wound management abilities which include: reducing pressure and shear forces; absorbing exudates; maintaining a moist environment; protection from trauma and bacterial invasion; and providing thermal insulation. In 2011, Witthayaprapakorn suggested 2-acrylamido-2-methylpropane sulfonic acid (AMPS) based hydrogels were suitable for use as burn wound dressings [19]. The study of water properties of the hydrogels (adsorption retention and water vapor transmission rate) indicated that they may have the ability to maintain moisture in the wound area. UV irradiation was performed to crosslink the polymer chains; however as UV irradiation is not a recommended sterilization technique for drugs and medical devices [20], the hydrogels were unfortunately not a ready-to-use dressing for medical purposes. Autoclaving is a recommended sterilization technique, however the impact of heat may cause changes in the polymer network and degradation of the dressing may occur.

In this study, we developed novel wound dressings comprised of the beneficial combination of AMPS sodium salt hydrogels containing SNP. The hydrogel promotes wound healing with

a moist environment and the SNP is lethal to pathogens that infect burns. The gamma irradiation technique used in this study serves as a single step synthesis of silver hydrogel dressings resulting in a ready-to-use sterile wound dressings. The antimicrobial activity of the novel dressings against common burn wound pathogens compared to commercially available silver dressings (product B and C) were evaluated using bactericidal measurement (broth culture and plate count method) in our previous study [21]. The cytotoxicity assessment of the novel dressings on human skin cell lines compared to common silver products (product B, C and Flamazine™ cream) was performed utilizing various cytotoxicity assays and was reported elsewhere [22]. This study details the preparation and characterization of the novel dressing and testing in an *in vivo* animal study. Pretests of antimicrobial activity and cytotoxicity compared to the commercial hydrogel (product A) were performed initially to select the best concentration of silver hydrogel for use in the animal study.

EXPERIMENTAL

Materials

2-acrylamido-2-methylpropane sulfonic acid (AMPS) was purchased from Merck Chemicals, Darmstadt, Germany. *N-N'*-methylenebis(acrylamide) (MBA) was purchased from Sigma-Aldrich, USA. Silver nitrate ($AgNO_3$) (99.998% purity) was purchased from Fisher Scientific, USA. Anhydrous sodium hydroxide (NaOH) pellets were of analytical grade and purchased from Carlo Erba, Milan, Italy. All other chemicals were of analytical reagent grade and used without further purification. The commercial dressings Cutinova Hydro® (a polyurethane gel matrix with a polyurethane film top), Acticoat™ (an absorbent polyester core laminated between two outer layers of nanocrystalline silver coated polyethylene mesh) and Jelonet® (an open weave gauze impregnated with soft paraffin) were purchased from Smith & Nephew (Hull, UK). PolyMem Silver® (a superabsorbent, hydrophilic polyurethane foam with surfactant, humectant and nanocrystalline silver) was obtained from Ferris Mfg Corp (USA). In this study, the commercial dressings were defined as product A, product B, product C and control product (Jelonet®).

Synthesis of AMPS hydrogels containing SNP

To create the silver hydrogel, AMPS monomer was dissolved in distilled water. The solution was titrated with NaOH solution under cold conditions to pH 7.0 ± 0.1 and the volume was adjusted to obtain a 40% (w/v) AMPS-Na^+ aqueous solution. The crosslinker, MBA (0.1%

mol/mol monomer) was added to the solution and the solution was stirred overnight at room temperature. To incorporate SNP into the hydrogel, $AgNO_3$ was dissolved in the AMPS-Na^+ aqueous solution in the presence of MBA to concentrations of 2.5 mM, 5 mM and 10 mM. The mixture was loaded into a nylon bag (0.2 ml of solution: 1 cm^2 surface area of the bag) and the contents were sealed and irradiated in a cobalt-60 gamma irradiator (IR-211, Nordion International Ltd., Ottawa, Ontario, Canada) at 25 kGy for 4.5 h. The pure or neat hydrogel was similarly produced without addition of $AgNO_3$.

Characterization of the SNP formation

The hydrogel sheets were air-dried and coated with a thin layer of palladium gold alloy. Surface morphology was monitored by scanning electron microscopy (SEM) using a Hitachi S-4800 (Chiyoda, Tokyo, Japan) operated at 3.0 kV and 20 μA. Hydrogels were submerged in deionized (DI) water at 35°C with agitation (60 rpm) for 24 h to obtain silver release solutions and these solutions were dried on copper grids. The particle sizes and crystal morphology were examined using transmission electron microscopy (TEM) on a FEI Tecnai G^2 F30 (USA) operated at 200 kV. Histograms of SNP size distribution were obtained from manually measuring the size of 200 particles from TEM images by the via ImageJ program version 1.47. Aliquots of the silver release solution from the hydrogels were mixed with a 1 M Hydrochloric acid solution (HCl). The mixtures were centrifuged to observe silver chloride (AgCl) precipitation.

Characterization of the physical properties of the hydrogels

The physical properties of the novel hydrogels were compared to product A. To determine the Equilibrium Degree of Swelling (EDS), each hydrogel was cut into 1.0 x 1.0 cm^2 pieces and was weighed (w_1), before being immersed in simulated body fluid solution (SBF) [23] at 35°C with agitation (60 rpm) for 72 h. The swelled hydrogels were then blotted and weighed (w_2) and the percent EDS was calculated as follows:

$$\text{EDS}\ (\%) = \frac{W2-W1}{W1} \times 100\ \%$$

To assess the gel fraction or percent gelation, the hydrogels were cut into 0.5 x 0.5 cm^2 pieces and dried in an oven at 60°C for 24 h to obtain the original dry weight (w_0). Each dried specimen was placed in a tea bag which was submerged in DI water at 121°C for 4 h in an

autoclave. The hydrogels were then dried at 60°C for 72 h to obtain the weight after extraction (w_E). The percentage of gelation was calculated using the following formula:

$$\text{Gelation } (\%) = \frac{W_E}{W_0} \times 100 \ \%$$

To determine the swelling ratio, the hydrogels were cut into 0.5 x 0.5 cm^2 pieces and dried in an oven at 60°C for 24 h to obtain the dry state weight (w_d), before being immersed in SBF solution at 35°C in a water bath with a shaking rate of 60 rpm. At the time intervals (0.5, 1, 2, 3, 6, 12, 24, 30, 72 h), the samples were removed from the solution, blotted and weighed to find the swollen state weight (w_s). They were then returned to the solution until equilibrium was reached. The swelling ratio was calculated by the following equation:

$$\text{Swelling ratio } (\%) = \frac{Ws - Wd}{Wd} \times 100 \ \%$$

To examine absorptive capacity, each hydrogel was cut into 1.0 x 1.0 cm^2 pieces and immersed in 30 ml of SBF at 35°C with agitation (60 rpm) for 1, 3, 6, 12, 24 or 72 h. After each time interval, the volume of the immersion solution was measured for evaluation of the absorptive capacity of the hydrogels.

To measure moisture retention, each hydrogel was cut into 0.5 x 0.5 cm^2 pieces, weighed (w_i) and placed in an oven at 35°C. At different time intervals (0, 3, 6, 12, 24, 72 h) the hydrogel was weighed (w_t) and moisture retention capability (R_h) was calculated using the following equation:

$$\text{Rh}(\%) = \left(\frac{Wt}{Wi}\right) \times 100\%$$

The measurement of water vapor transmission rate (WVTR) was conducted according to a monograph of the European Pharmacopoeia [24]. A hydrogel disc (15 mm in diameter) was used to cover the top of a 13 mm diameter bottle (A = area of the bottle mount in m^2) containing 10 ml of DI water. Parafilm was used to seal between the top of the bottle and the hydrogel. The WVTR of the hydrogel was determined by measuring the weight of the bottle before (w_i) and after (w_t) being kept in an oven at 35°C for 24 h, and was calculated using the following formula:

$$WVTR = \frac{(Wi\text{-}Wt)}{A \times 24} \times 10^6 \quad g.\ m^{-2}\, h^{-1}$$

Characterization of the mechanical properties of hydrogels

The tensile strength and elongation at breaking point of the hydrogel were measured using 5.0 cm x 1.0 cm pieces on a universal testing machine (Lloyd LRX, Lloyd Instruments Ltd, Fareham, Hampshire, UK) with a 500 N load and a cross-head speed of 50 mm/min.

Study of silver release from the silver hydrogels

To assess the cumulative silver released under physiological conditions the silver hydrogels were cut into 15 mm diameter discs, and each disc was immersed in 50 ml SBF solution at 35°C with agitation at 60 rpm. At various time intervals (1, 3, 6, 12, 24 h, 3, 5, 7, 10 days), the immersion solution was collected to measure the silver content and the 50 ml SBF solution was replaced at each time interval. The concentration of silver, either in neutral or ion form, was measured by atomic absorption spectroscopy using a flame atomic absorption spectrometer (SpectrAA300, Varian, USA). To measure the actual amount of silver within the hydrogel, the same size disc was immersed in 50 ml of nitric acid (HNO_3) to extract the silver from the dressing. The total silver in the solution was then examined.

Cytotoxicity of the hydrogels

The cytotoxicty evaluation was based on a protocol adapted from the ISO 10993-5 [25] standard test method. Neat hydrogel, silver hydrogels and product A were cut into 5 mm diameter discs and sterilized by immersion in 70% v/v ethanol for 30 min. They were then washed twice with 10 mM phosphate buffered saline (PBS, pH 7.4) and DI water before being immersed in 24-well tissue-culture polystyrene plates (TCPS; NunclonTM, Roskilde, Denmark) that contained 2 ml of a serum-free media (SFM) of Dulbecco's Modified Eagle Medium (DMEM) containing 1% l-glutamine, 1% lactalbumin, and 1% antibiotic and antimycotic formulation (Invetrogen Corp., USA) for 1, 3 and 7 days. After these time points, the hydrogels were removed and the extraction media were collected.

Normal human dermal fibroblast (NHDF) cells were cultured in DMEM media (comprised of 10% fetal bovine serum (FBS), 1% l-glutamine, and 1% antibiotic and antimycotic (Invitrogen Corp., USA) at 37°C with media changed every 3 days. The cells were seeded in a 24-well plate at a density of 10,000 cells/well in DMEM overnight to allow cell attachment.

The media was replaced with SFM for the next 24 h and then the hydrogel extraction media for 24 h.

The relative cell viability was determined using a 3-(4, 5-dimethylthiazol-2-yl)-2, 5-diphenyltetrazolium bromide (MTT, Sigma, USA) assay. After a PBS (10 mM, pH 7.4) wash, 300 µl of 0.5 mg/ml MTT was added to each well and cells were incubated at 37°C for 30 min before removal of MTT solution. Yellow MTT is reduced to purple formazan crystals in the mitochondria of living cells [26]. The purple crystals were dissolved in 1 ml of dimethylsulfoxide (DMSO) solution (9:1.25 v/v of DMSO:glycine buffer pH 10.5). The plate was agitated for 10 min at 250 rpm and absorbance at 570 nm was measured on a Thermospectronic Genesis 10 UV-vis spectrophotometer (Thermo Spectronic, USA). Three independent experiments were performed for the cytotoxicity assay. Differences between samples and controls were evaluated with one-way analysis of variance (ANOVA) and the Tukey's Multiple Comparison Test using GraphPad Prism version 6.03. Statistically significant differences were set at $p < 0.01$ (99% confidence).

Measurement of antibacterial activity by the disc diffusion method

The hydrogels were immersed in DI water for 24 h to prevent absorption of water from the agar. They were then cut into discs (5 mm diameter) and sterilized under a Funa-UV-Linker FS800 (Funakoshi, Bunkyo-ku, Tokyo, Japan) for 30 min. The disc diffusion method described by The US Clinical and Laboratory Standards Institute (CLSI) [27] was used with common burns pathogens: three gram positive bacteria (*Staphylococcus aureus* ATCC 25923, *Staphylococcus Epidermidis* wild type, and Methicillin-resistant *Staphylococcus aureus* (MRSA) wilde type) and two gram-negative bacteria (*Escherichia coli* ATCC 25922, *Pseudomonas aeruginosa ATCC 9027*). To simulate an infected wound, a microbial load greater than 10^5 colony forming unit (CFU)/g of tissue [28] is required, so the bacterial colonies were diluted in normal saline to a 0.5 McFarland Standard solution (10^8 CFU/ml). The bacteria inocula were spread on Tryptic Soy Agar (TSA) plates and the hydrogel discs were placed on the agar. Plates were incubated at 37°C for 24 h and the diameter of the inhibition zone was measured for each hydrogel disc.

Measurement of antibacterial activity by the shake flask method

A shake flask method modified from ASTM E2149-01 was used to test activity against two major pathogens that infected burn wounds: gram-positive MRSA (wild type) and gram-negative *P. aeruginosa* (ATCC 9027). Glassware and solutions were sterilized in an autoclave

at 121°C for 15 min before being used and the test samples were cut into 15 mm diameter discs and sterilized under UV lamps for 30 min. A colony of *P. aeruginosa* or MRSA was cultured in 2 ml of Tryptic Soy Broth (TSB) at 37°C for 2 h with agitation (Orbital incubator shaker, GYROMAX^{TM} 737, Amerex Inst. Inc., USA) at 250 rpm. The culture medium was transferred to a 100 ml of TSB and incubated for 3-5 hours with shaking at 250 rpm until the optical density at 600 nm (OD 600) was 0.2 - 0.3. The cells were then isolated using a refrigerated microcentrifuge (Kubota-6500, Kubota Crop. Bunkyo-ku Tokyo, Japan) at 8000 rpm, 4°C for 10 min. The cells were washed with normal saline solution and were diluted with alkaline peptone water (APW) to create a 5 ml culture medium solution with a cell concentration of 10^8 CFU ml. Addition of 200 µl of this diluted cell culture solution into a flask that contained 50 ml of APW created a solution of 10^6 CFU/ml of cells. Each hydrogel sample was then added to individual culture flasks, which were incubated at 37°C on a shaker (250 rpm). At each time point (0, 1, 3, 6, 12, 24 h), a 0.5 ml aliquot underwent serial tenfold dilutions (10^{-1},10^{-2},10^{-3},…) and 100 µl of each diluted solution was spread on duplicate TSA plates. The plates were incubated for 24 h at 37°C, and the average number of colonies was expressed as CFU/ml after correction for the dilution factor. Bacterial surviving curves were plotted using the number of colonies at each culture time point. The log reduction compared to an untreated culture was also calculated using the following equation:

$$\text{Log reduction} = \text{Log (CFU.ml}^{-1}\text{ of control)} - \text{Log (CFU.ml}^{-1}\text{ of sample)}$$

A pilot study on a porcine burn model

The animal experiment was approved by the University of Queensland Animal Ethics committee and the animal was treated humanely and with appropriate analgesics. One young Large White juvenile pig weighing 26 kg (approximately 8 weeks old) was used for this study. Wounds were created under general anaesthesia using a modified version of method developed from our previous research involving deep dermal partial thickness burn injury in pigs [29]. Four of these wounds were created on each flank, with 8 wounds in total. Four different treatments including: the control product with Melolin® (Smith & Nephew, Hull, UK) on top, product B, product C and 5 mM silver hydrogel with Tegaderm^{TM} film (3M, USA) on top were randomly applied on the 8 wounds in duplicate. The size of each dressing was 5x5 cm^2. Dressings were changed every 2-3 days. Wounds were photographed and clinical notes were taken to record the healing process. At the end of week 6, five examiners recorded the appearance of the treated wounds as a cosmetic score before the animal was

euthanized. Statistical analysis of the cosmetic score was performed according to a method similar to that described for cytotoxicity study.

RESULTS AND DISCUSSION

Silver nanoparticle formation

The gamma irradiation technique used in this study serves as a single step synthesis of silver hydrogel dressings. It was used to crosslink the polymer chains, to reduce silver ions to form SNP, and to provide ready-to-use sterile wound dressings. Figure 1 shows a schematic representation of radical polymerization of AMPS monomer in the presence of an MBA crosslinker and the reduction of silver ions to form SNP infused in the crosslinked polymer network due to gamma irradiation. Gamma irradiation generates solvated electrons and hydrogen radicals, which reduce silver ions to neutral silver atoms that consequently coalesce to form SNP [30, 31]. The original colorless AMPS sodium salt solution created colorless neat hydrogels. Gamma irradiation changed the colorless silver AMPS sodium salt solutions into brown hydrogels, with darker shades of brown resulting from increased concentrations of silver (Figure 2). A similar observation was also reported elsewhere [32]. SEM images reveal that the pure hydrogel had a plain smooth surface while silver hydrogels had rough surfaces with particles on the surfaces (Figure 3b-c). Similar results were observed in a previous study [33]. The SEM image of 10 mM silver hydrogel (Figure 3c) shows denser distribution of particles than the SEM image of 5 mM silver hydrogel (Figure 3b). The TEM images of the silver released from the hydrogels indicated that the size of the SNP were less than 30 nm (Figure 4a-c). The histograms of particle size distributions of the silver hydrogels obtained from the corresponding TEM images are shown in Figure 4a-c. The average particle sizes were 8.08, 6.53, 4.83 nm for 2.5, 5 and 10 mM silver hydrogel, respectively. The 10 mM silver hydrogel was found the have the most uniform size distribution with 3-6 nm SNP at 57.5% abundance. Figure 4d shows TEM images of selected single crystals of SNP released from 5 mM silver hydrogel. The particles were crystalline in variety of shapes. Similarly, a variety of single crystal shapes was observed from the SNP released from 2.5 and 10 mM silver hydrogel (images not shown).

SNP are generally unstable in suspension and can be readily oxidized and dissolved into silver ions [17]. The novel silver hydrogels would therefore be expected to contain a proportion of ionic silver which was not completely transformed into SNP during the hydrogel preparation process. The silver release solutions from the hydrogels were mixed with HCl solution in order to observe silver chloride (AgCl) precipitation and therefore the presence of ionic silver. Unpredictably, no precipitation was visually observed. This may be due to a very low concentration of silver ions dissolved into the solution, indicating the majority of silver in the dressing is present as SNP.

Characterization of hydrogel physical and mechanical properties

The EDS of the neat hydrogel was 1278.6% (Table 1). The EDS decreased from 1478.1% to 1228.4% as the silver concentration increased from 2.5 to 10 mM. These EDS values were inversely proportional to the gelation values (72.1% for 2.5 mM, 80.7% for 5 mM and 82.7% for 10 mM). Gelation inversely relates to the free volume inside the gel networks, with 2.5 mM silver hydrogel displaying the lowest gelation or highest free volume inside the gel and the highest EDS. The EDS of product A was 443.1%, which is about 3 times lower than the AMPS hydrogels and the gelation of product A was 95.8%, indicating the low free volume inside the gel networks.

After 72 h of immersion in SBF solution, AMPS hydrogels had a calculated absorptive capacity of 6.3-7.3 ml/cm^2 of hydrogel (surface area), compared to the calculated absorptive capacity of product A at 72 h, which was 4.6 ml/cm^2 of hydrogel (Table 1). This indicated that all of the AMPS hydrogels have greater ability to adsorb exudate from wounds than the commercial hydrogel. The results confirmed an earlier report that product A had a lower free volume in the gel network than AMPS hydrogels and, therefore, it had less adsorption capacity.

The moisture retention results at 6 h did not show any significant difference in values between the neat and silver hydrogel (Table 1). Moisture retention capacity of the neat and silver hydrogels ranged between 97.5-98.1 %, confirming that the neat hydrogel and the silver hydrogels had the same moisture retention. Product A had a moisture retention capacity of 100.1%, indicating that none of the water evaporated from the commercial hydrogel within 6 h at 35°C.

The WVTR values of all hydrogels (range 86.7-102.0 g.h^{-1}.m^2, Table 1) were lower than the evaporative water loss of second and third degree burned skin (178 ± 5.5 g/h.m^2 and 143.2 ± 4.5 g/h.m^2, respectively) [34]. This suggests that the AMPS hydrogels can be used to retain

body fluid and preserve a moist environment for burn wounds. Product A had an extremely low WVTR value (0.94 ± 0.5 g/h.m^2) which was lower than first degree burn (8.5 ± 0.5 g/h.m^2) [34] as well as second and third degree burned skin. This result indicates that product A would have a greater ability than the developed novel silver hydrogel to protect against water loss and maintain a moist environment for all degrees of burn wounds, particularly superficial burns.

All silver hydrogels initially showed an accelerated increase in swelling until 12 h (Figure 5), with equilibrium reached at 72 h. The concentration of silver affected the swelling behaviors of the hydrogels. The 2.5 mM silver had the highest swelling capacity at each time interval, followed by 5 mM and 10 mM, respectively. For the EDS and percent gelation, it would be expected that the greater the concentration of silver, the less free volume of the hydrogel network available to absorb water. Unexpectedly, the neat hydrogel had swelling behavior, EDS values and percent gelation, similar to the 10 mM silver hydrogel. It can be hypothesized that without SNP, pure AMPS hydrogels have a different network configuration due to the presence of Na^+ ions. The gel network structures of these dressings should be examined in future studies.

The mechanical properties of the hydrogel wound dressings were assessed by tensile strength and elongation at breaking point (Table 1). All silver loaded hydrogels had tensile strength values (0.0280-0.0328 MPa) similar to the neat hydrogel (0.0294 MPa). The tensile strength of product A was greatest (0.0419 MPa). The elongation at breaking point for all silver loaded hydrogels (222.3%-253.3%) was higher than the neat hydrogel (183.5%). For product A the elongation at break point was 765.3% or about 3 fold higher than the AMPS hydrogels.

Cumulative silver release

The amount of silver released from the silver hydrogels when submerged in SBF or HNO_3 solution is shown in Table 2. The cumulative silver released from silver hydrogels after 10 days of immersion in SBF were 90.25%, 89.97% and 81.26% for 2.5 mM, 5 mM and 10 mM silver, respectively. The release of silver from the hydrogels could be divided into three stages (Figure 6). During the initial 24 h of immersion time, there was rapid release of about 60% of the total silver released. From 24 h - 72 h, the cumulative releases of silver were 82.41%, 75.63% and 78.56% for 2.5 mM, 5 mM and 10 mM silver hydrogels, respectively. A slight but continuous terminal silver release from 72 h - 240 h was observed for all of the hydrogels. A time course of silver release solution from the hydrogels (1, 3, 6, 24, 72 h) was also observed using TEM. This showed that more SNP were released with longer immersion

times, confirming silver is released from the dressings as SNP, rather than ions. It can be concluded that the hydrogels when used as a wound dressing, would be actively releasing silver over 72 h.

Cytotoxicity evaluation

NHDF cells were treated with the extraction media from the neat hydrogel, silver hydrogels and product A, and cell viability was assessed at 1, 3 and 7 days (Figure 7). This was considered an indirect cytotoxicity assessment, because the extraction media of the hydrogel samples were tested on the cells instead of the hydrogel samples directly. None of the hydrogel samples were identified as toxic to NHDF as after all treatments, cells had over 90% viability. There was no significant difference ($p > 0.01$) in cell viability of all test hydrogels compared to controls up to 7 days confirming that the hydrogels have no cytotoxicity to the tested cells. Similar results were observed in our previous study of intensive cytotoxicity assessment of the hydrogels compared to topical silver products used in burn care on different skin cell lines [22].

Antibacterial evaluation

The inhibition zone diameters of bacteria after treatment with the 5 mm diameter hydrogels and product A pre-swelled in DI water are shown in Table 3. For the neat hydrogel and product A, no antibacterial activity was observed after treatment for 24 h. The 2.5 mM silver hydrogel had antibacterial activity against *E.coli* but not against any of the other bacteria. The 10 mM silver hydrogel had the most powerful inhibitory activity for all bacteria tested, and 5 mM silver hydrogel also inhibited the cell growth of all bacteria. However, this experiment was performed with swelled hydrogels (immersion in DI water for 24 h to prevent absorption of water from the agar) and possibly over 60% of the silver infused in the hydrogels may have already been released from the hydrogels during the pre-immersion according to the silver release study. Consequently, the swelled silver hydrogels may have lost some antibacterial activity before the treatment.

As the 2.5 mM hydrogel showed poor inhibitory activity in the disc diffusion method, it was excluded from the shake flask experiment. The log reduction of bacterial cell growth of bacterial inocula of 10^6 CFU/ml treated with the neat hydrogel, silver hydrogels (5 mM and 10 mM silver) and product A at different time intervals are shown in Table 4. The bacterial survival curves of *P. aeruginosa* and MRSA are shown in Figure 8a and 8b, respectively. For gram-negative *P. aeruginosa*, 5 mM and 10 mM silver hydrogels had a similar potential to

inhibit the bacteria cell growth. After 3 h treatment, the log reduction was >4.43. A log reduction >3 is referred to bactericidal whereas log reduction <3 is considered bacteriostatic [21, 35]. Therefore, the results indicate that 5 and 10 mM silver hydrogels are bacteriocidal at 3 h against *P. aeruginosa.* These results were also graphed as survival curves (Figure 8a). After 3 h, both silver hydrogels reduced the microbe inocula below the detection limit (10^2 CFU/ml). For MRSA, 5 mM and 10 mM silver hydrogel inhibited the bacterial cell growth after 12 h of treatment, with a log reduction of >6.41. Both 5 mM and 10 mM silver hydrogels reduced the tested microbial inocula below the detection limit within 12 h (Figure 8b). Wang *et al* [36] has previously reported two explanations as to why gram-positive bacteria may be less susceptible to silver ions than gram-negative bacteria. First, silver ions are positively charged and more silver may get trapped by the negative charge of the peptidoglycan cell wall in gram-positive bacteria. Second, the fact that the cell wall of gram-positive bacteria is thicker than that of gram-negative bacteria may lead to the decreased susceptibility of gram-positive bacteria. In the case of the neat hydrogel and product A, log reductions fluctuated considerably indicating poor inhibition activity. The survival curves of both microbes treated with these hydrogels showed they were never able to reduce the colony level to below 10^5 CFU/ml.

Treatments on a porcine burn model

The 5 mM silver hydrogel was chosen to be the best dressing and was used for testing in an animal study due to it having the least silver content required for effective antibacterial activity. A porcine model was selected due to morphological and physiological similarities to human skin [29]. This pig burn model mimics human clinical wounds in appearance, exudate, breakdown, scarring and healing process. Large bacteria colonization zones were observed for both control wounds. Small red bumps were found around the wounds as shown in Figure 9a. A skin swab was not collected, however skin rashes of this nature have been identified from previous animals undergoing wound healing studies as being colonised with *Staphylococcus*. The wounds treated with silver hydrogel (Figure 9b) and the commercial silver dressings (product B and product C) showed no bacterial colonization. This is in accordance with the theory that silver incorporated in dressings helps to prevent wound infection. Product B treatments left a stain from the released silver. The visible stain from treatment of product B may due to the fact that product B has a silver content of 0.84-1.34 mg/cm^2 [37] which is about 10 fold higher than the silver content in the 5 mM silver hydrogel (maximum silver content of 0.108 mg/cm^2). The wound exudate, which was absorbed into the dressing, was

found to increase the chance of breakage of product C and the silver hydrogel. The silver hydrogel was found to be an easily removable dressing (Figure 9d). Its transparency enabled observation of the wound healing process (Figure 9c). In addition, it efficiently absorbed the exudate from the wound. The hydrogel darkened in color due to exudate adsorption. All wounds took approximately 35 days to completely re-epithelize. The cosmetic scores for all the wounds treated with silver dressings were not significantly different ($p > 0.01$) compared to the control wound. It can be concluded that silver hydrogel was comparable to the common silver dressings tested. Additionally, there are three particular advantages of the developed silver hydrogel over the commercially available dressings tested. Firstly, the single step synthesis provides a ready to use sterile dressing. Secondly, it is non-cytotoxic, yet has strong antimicrobial activity. Finally, the low-cost novel dressing which is easy and cheap to manufacture can be a good treatment option for developing countries and rural locations.

CONCLUSIONS

Novel antibacterial burn wound dressings based on AMPS-Na^+ hydrogel containing SNP have been successfully prepared with single step production via gamma irradiation. The formation of SNP was confirmed by electron microscopy. The WVTR confirmed that all hydrogels could be used to decrease body fluid loss and maintain a moist environment for burn wounds. The cumulative release of silver from the novel dressings was about 80% at 72 h. Therefore, it would be an effective antimicrobial wounds dressing for approximately 72 h. The cytotoxicity test results showed that none of the silver hydrogels were toxic to NHDF for at least 7 days of exposure. The antibacterial activity evaluation indicated that the 5 mM and 10 mM silver hydrogels inhibited the growth of gram-positive MRSA after 12 h of the treatment and they took only 3 h to inhibit gram-negative *P. aeruginosa* cell growth. The 5 mM silver hydrogel was selected to be the best dressing and was used to treat a porcine burn model in comparison to the two common silver burn wound dressings (product B and product C). All silver treatments sufficiently protected the wounds from bacterial colonization. The cosmetic score revealed the novel silver hydrogel was a comparable dressing to the two common dressings. The simple production, effective antimicrobial activity, lack of cytotoxicity and effective use in an animal study support the use of the 5 mM silver hydrogel as a novel burn wound dressing.

CONFLICT OF INTEREST

The author B. Boonkaew is involved in a patent application for the novel hydrogel. The other authors have no conflict of interest regarding the novel dressing.

ACKNOWLEDGEMENTS

The authors acknowledge Prof. Roy M. Kimble who provided the research facilities at the Centre for Children's Burns and Trauma Research, Queensland Children's Medical Research Institute, The University of Queensland, Queensland, Australia. Cytotoxicity assessment was performed at the Department of Anatomy, Faculty of Dentistry, Chulalongkorn University, Thailand with support from Prof. Prasit Pavasant. Suggestions and comments on the burn dressings were received from Dr. Angkana Tanvatanagul and the nurses at the burn center, Nopparat Rajathanee Hospital, Thailand. Blair McEwan and Brad Buchan are technicians at Herston Medical Research Centre (HMRC), Royal Children's Hospital, Australia who assisted with the animal experiments. The postdoctoral scholarship for B. Boonkaew was received from the Development and Promotion of Science and Technology Talents Project (DPST).

REFERENCES

[1] Silvestry-Rodriguez N, Sicairos-Ruelas EE, Gerba CP, Bright KR 2007. Silver as a disinfectant. Rev Environ Contam Toxicol 191:23-45.

[2] Moyer CA, Brentano L, Gravens DL, Margraf HW, Monafo WW Jr 1965. Treatment of large human burns with 0.5 percent silver nitrate solution. Arch Surg 90:812-867.

[3] Fox CL Jr 1968. Silver sulfadiazine-a new topical therapy for *Pseudomonas* burns. Arch Surg 96:184-188.

[4] Fox CL Jr, Modak S 1974. Mechanism of silver sulfadiazine action on burn wound infections. Antimicrob Agents Chemother 5:582-588.

[5] Guggenbichler JP, Boswald M, Lugauer S, Krall T 1999. A new technology of microdispersed silver in polyurethane induces antimicrobial activity in central venous catheters. Infection 27:S16-S23.

[6] Dunn K. Edwards-Jones V 2004. The role of Acticoat with nanocrystalline silver in the management of burns. Burns 30:S1-S9.

[7] Gordon O, Vig Slenters T, Brunetto PS, Villaruz AE, Sturdevant DE, Otto M, Landmann R, Fromm KM 2010. Silver coordination polymers for prevention of implant infection: thiol interaction, impact on respiratory chain enzymes, and hydroxyl radical induction. Antimicrob Agents Chemother 54:4208-4218.

[8] Yakabe Y, Sano T, Ushio H, Yasunaga T 1980. Kinetic studies of the interaction between silver ion and deoxyribonucleic acid. Chem Lett 4:373-376.

[9] Yin HQ, Langford R, Burrell RE 1999. Comparative evaluation of the antimicrobial activity of ACTICOAT antimicrobial barrier dressing. J Burn Care Rehabil 20:195-200.

[10] Rai M, Yadav A, Gade A 2009. Silver nanoparticles as a new generation of antimicrobials. Biotechnol Adv 27:76-83.

[11] Fong J. Wood F 2006. Nanocrystalline silver dressings in wound management: a review. Int J Nanomedicine 1:441-449.

[12] Ong SY, Wu J, Moochhala SM, Tan MH, Lu J 2008. Development of a chitosan-based wound dressing with improved hemostatic and antimicrobial properties. Biomaterials 29:4323-4332.

[13] Jain J, Arora S, Rajwade JM, Omray P, Khandelwal S, Paknikar KM 2009. Silver nanoparticles in therapeutics: development of an antimicrobial gel formulation for topical use. Mol Pharmaceutics 6:1388-1401.

[14] Martinez-Castanon GA, Nino-martinez N, Martinez-Gutierrez F, Martinez-Mendoza JR, Ruiz F 2008. Synthesis and antibacterial activity of silver nanoparticles with different sizes. J Nanopart Res 10:1343-1348.

[15] Oza G, Pandey S, Shah R, Sharon M 2012. Extracellular fabrication of silver nanoparticles using pseudomonas aeruginosa and its Antimicrobial Assay. Adv Appl Sci Res 3:1776-1783.

[16] Egger S, Lehmann RP, Height MJ, Loessner MJ, Schuppler M 2009. Antimicrobial properties of a novel silver-silica nanocomposite material. Appl Environ Microbiol 75:2973-2976

[17] Reidy B, Andreas H, Luch A, Dawson KA, Lynch I 2013. Mechanisms of silver nanoparticle release, transformation and toxicity: A critical review of current knowledge and recommendations for future studies and applications. Materials 6:2295-2350.

[18] Li Q, Mahendra S, Lyon DY, Brunet L, Liga MV, Li D, Alvarez PJ 2008. Antimicrobial nanomaterials for water disinfection and microbial control: Potential applications and implications. Water Res 42:4591-4602.

[19] Witthayaprapakorn C 2011. Design and preparation of synthetic hydrogels via photopolymerisation for biomedical use as wound dressings. Procedia Eng 8:286-291

[20] Silindir M, Ozer AY 2009. Sterilization methods and the comparison of e-beam sterilization with gamma radiation sterilization. FABAD J Pharm Sci 34:43-53.

[21] Boonkaew B, Kempf M, Kimble R, Supaphol P, Cuttle L 2014. Antimicrobial efficacy of a novel silver hydrogel dressing compared to two common silver burn wound dressings: Acticoat™ and PolyMem Silver®. Burns 40:89-96.

[22] Boonkaew B, Margit K, Kimble R, Supaphol P, Cuttle L 2014. Cytotoxicity testing of silver-containing burn treatments using primary and immortal skin cells. Burns. in press:doi.org/10.1016/j.burns.2014.02.009

[23] Kokubo T, Kushitani H, Sakka S, Kitsugi T, Yamamuro T 1990. Solutions able to reproduce in vivo surface-structure changes in bioactive glass-ceramic A-W. J Biomed Mater Res 24:721-734.

[24] Arya A, Sharma V, Pathak K 2013. Pharmaceutical evaluation and dynamic vapor sorption studies of fast dissolving intraoral films of Loratadine. Pharmaceut Dev Tech 18:1329-1338.

[25] International Organizatin for Standardization 2009. International standard ISO10993-5 , Biological evaluation of medical deviced-Part 5: Test for *in vitro* cytotoxicity. ISO, p 24-28.

[26] Mosmann T 1983. Rapid colorimetric assay for cellular growth and survival: application to proliferation and cytotoxicity assays. J Immunol Methods 65:55-63.

[27] Clinical and Laboratory Standards Institute 2005. Methods for antimicrobial dilution and disk susceptibility testing of infrequently isolated or fastidious bacteria; proposed guideline. CLSI document M45-P (ISBN 1-56238-583-6). Pennsylvania: Clinical and Laboratory Standards Institute

[28] Bowler PG, Duerden BI, Armstrong DG 2001. Wound microbiology and associated approaches to wound management. Clin Microbiol Rev 14:244-269.

[29] Cuttle L, Kempf M, Phillips GE, Mill J, Hayes MT, Fraser JF, Wang XQ, Kimble RM 2006. A porcine deep dermal partial thickness burn model with hypertrophic scarring. Burns 32:806-820.

[30] Zheng J, Clogston JD, Patri AK, Dobrovolskaia MA, McNeil SE 2011. Sterilization of silver nanoparticles using standard gamma irradiation procedure affects particle integrity and biocompatibility. J Nanomedic Nanotechnol S5:001. :doi.org/10.4172/2157-7439.S5-001

[31] Li T, Park HG, Choi SH 2007. γ-Irradiation-induced preparation of Ag and Au nanoparticles and their characterizations. Mater Chem Phys 105:325-330.

[32] Rattanaruengsrikul V, Pimpha N, Supaphol P 2009. Development of gelatin hydrogel pads as antibacterial wound dressings. Macromol Biosci 9:1004-1015.

[33] Babu AC, Prabhakar MN, Babu AS, Mallikarjuna B, Subha MCS, Rao KC 2013. Development and characterization of Semi-IPN silver nanocomposite hydrogels for antibacterial applications. Int J Carbohydr Chem. in press:doi.org/10.1155/2013/243695

[34] Nilsson GE 1997. On the Measurement of Evaporative Water Loss, method and clinical application. Linkoping: Zata Tryerierna

[35] Hoellman DB, Pankuch GA, Appelbaum PC 2004. Antistaphylococcal activity of CB-181963 (CAB-175), an experimental parenteral cephalosporin. Antimicrob Agents Chemother 48:4037-4039.

[36] Wang L, Luo J, Shan S, Crew E, Yin J, Zhong CJ 2011. Bacterial inactivation using silver-coated magnetic nanoparticles as functional antimicrobial agents. Anal Chem 83:8688-8695.

[37] Arvidsson R, Molander S, Sanden BA 2011. Impacts of a silver-coated future. J Ind Ecol 15:844-854.

Table 1 Physical and mechanical properties of the tested hydrogels from triplicate experiments.

Sample	EDS (% at 72 h)	Gelation (%)	Adsorptive capacity (ml/cm^2)	Moisture retention (% R_h at 6)	WVTR ($g/m^2/h$) (72 h)	Tensile strength (MPa)	Elongation at break (%)
neat	1278.6 ± 19.5	84.6 ± 8.5	7.3 ± 0.6	98.1 ± 0.1	97.5 ± 5.0	0.0294 ± 0.0057	183.5 ± 68.7
2.5 mM	1478.1 ± 20.4	72.1 ± 9.8	7.1 ± 0.7	97.5 ± 0.1	102.0 ± 4.2	0.0280 ± 0.0030	222.3 ± 42.9
5 mM	1360.9 ± 5.9	80.7 ± 8.2	6.7 ± 0.2	97.7 ± 0.3	95.2 ± 4.9	0.0328 ± 0.0066	253.3 ± 66.5
10 mM	1228.4 ± 0.3	82.7 ± 9.3	6.3 ± 0.1	97.8 ± 0.2	86.7 ± 3.1	0.0296 ± 0.0038	232.5 ± 30.3
product A	443.1 ± 4.4	95.8 ± 0.4	4.6 ± 0.3	100.1 ± 0.1	0.94 ± 0.5	0.0419 ± 0.0046	765.3 ± 134.6

Table 2 Amount of extracted silver, amount of silver released and percentage of cumulative silver release of the silver hydrogels after 10 days immersion in SBF from triplicate experiments.

Concentration of silver (mM)	Amount of extracted silver (ppm)	Amount of silver released (ppm)	(%) cumulative silver release
2.5	1.95	1.76 ± 0.09	90.25 ± 4.65
5	3.09	2.78 ± 0.41	89.97 ± 13.27
10	6.62	5.38 ± 0.33	81.26 ± 5.01

Table 3 Inhibition zone length of bacteria treated with the hydrogels by the disc diffusion method from triplicate experiments.

sample	Inhibition zone length (mm)				
	S. aureus	MRSA	*S. epidermidis*	*E. coli*	*P. aeruginosa*
neat	0	0	0	0	0
2.5 mM	0	0	0	7.4 ± 0.6	0
5 mM	8.7 ± 0.6	8.2 ± 0.3	8.9 ± 0.4	8.4 ± 0.4	7.2 ± 0.8
10 mM	10.8 ± 0.7	8.9 ± 0.9	10.7 ± 0.7	10.4 ± 0.7	8.7 ± 0.7
product A	0	0	0	0	0

Table 4 Log reduction of MRSA and *P. aeruginosa* cell growth after treatment with the tested hydrogels using the shake flask method from duplicate experiments.

Bacteria	Hydrogels	Log reduction at time intervals (h)				
		1	3	6	12	24
P.aeruginosa	product A	0.40 ± 0.06	0.89 ± 0.28	0.34 ± 0.04	0.38 ± 0.02	1.34 ± 0.03
	neat	0.35 ± 0.02	0.28 ±0.03	0.02 ± 0.04	0.14 ± 0.07	1.15 ± 0.06
	5	1.33 ± 0.09	>4.43 ± 0.00	>5.21 ± 0.00	>6.68 ± 0.00	>7.26 ± 0.00
	10	1.75 ± 0.65	>4.43 ±0.00	>5.21 ± 0.00	>6.68 ± 0.00	>7.26 ± 0.00
MRSA	product A	-0.02 ± 0.09	0.01 ± 0.09	0.38 ± 0.01	1.57 ± 0.01	1.38 ± 0.34
	neat	-0.01±0.02	0.02 ± 0.01	0.66 ±0.10	0.69 ± 0.11	0.36 ± 0.00
	5 mM	0.01 ± 0.09	0.38 ±0.10	2.53 ± 0.10	>6.41 ± 0.00	>6.28 ± 0.00
	10 mM	-0.03 ± 0.08	2.60 ±0.05	3.02 ± 0.17	>6.41 ± 0.00	>6.28 ± 0.00

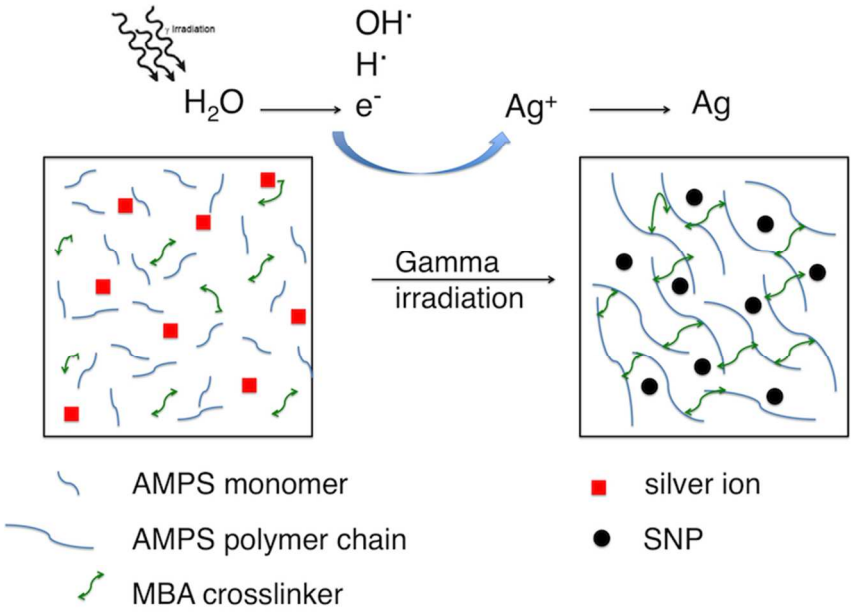

Figure 1. A schematic representation of polymerization of AMPS monomer with gamma irradiation. Silver ions were reduced to form SNP which were infused in the crosslinked polymeric network.
80x58mm (300 x 300 DPI)

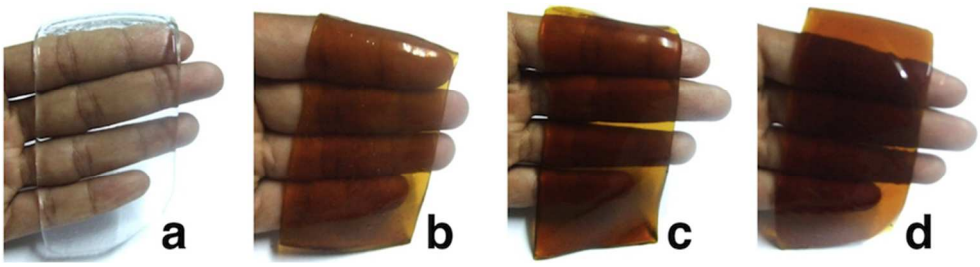

Figure 2. The appearance of the radiated hydrogel pads darkened with increasing silver concentration. a: neat hydrogel, b: 2.5 mM silver hydrogel, c: 5 mM silver hydrogel, d: 10 mM silver hydrogel.
80x20mm (300 x 300 DPI)

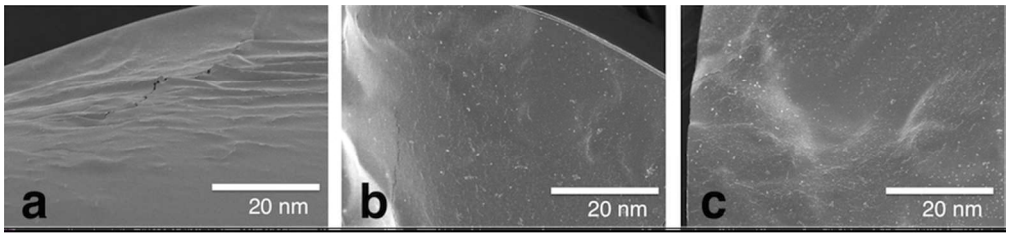

Figure 3. SEM images of a neat hydrogel, b: 5 mM silver hydrogel and c: 10 mM silver hydrogel.
80x18mm (300 x 300 DPI)

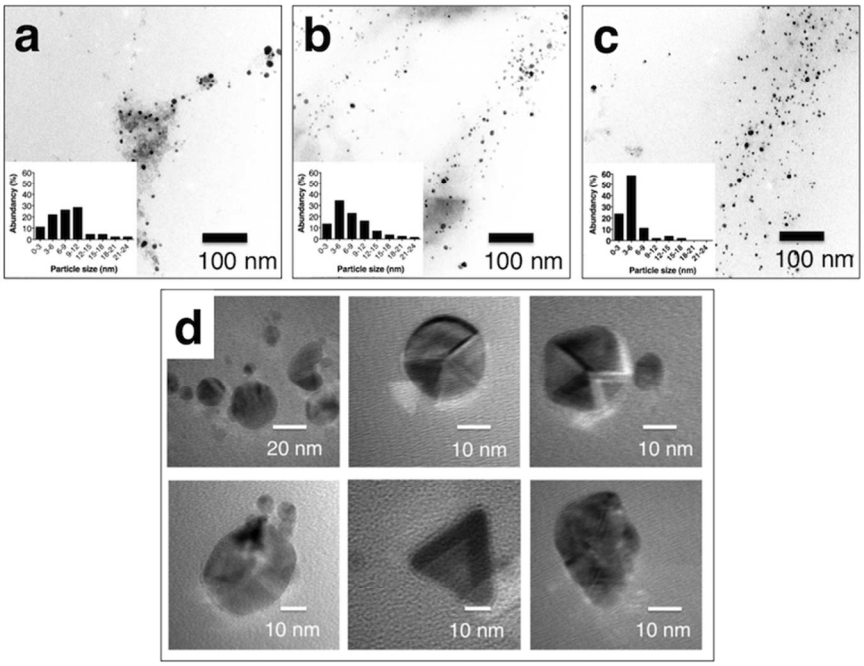

Figure 4. TEM images from immersion solutions of silver hydrogels and histograms of size distribution from the respective TEM images. a: 2.5 mM silver hydrogel, b: 5 mM silver hydrogel and c: 10 mM silver. d: TEM images of selected single crystals of SNP released from 5 mM silver hydrogel.
80x56mm (300 x 300 DPI)

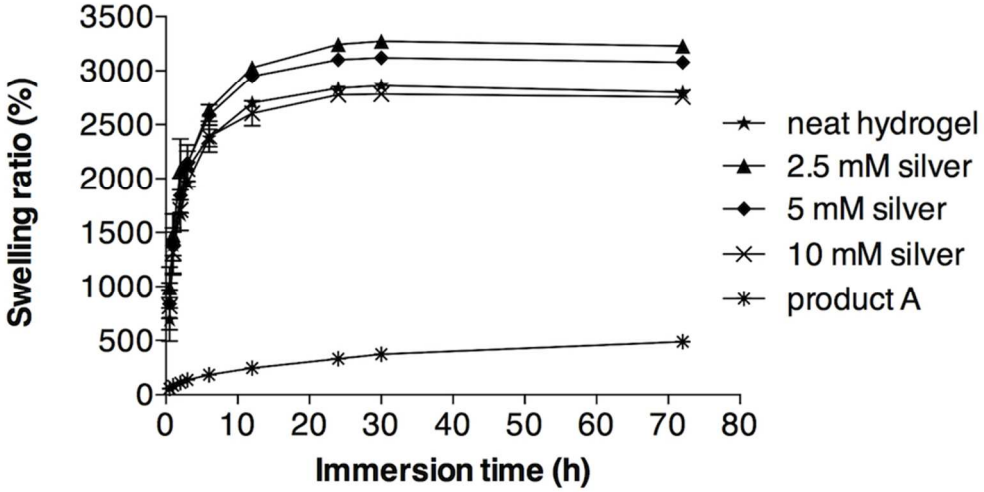

Figure 5. The swelling behaviors of the neat hydrogel, silver hydrogels and product A immersed in simulated body fluid solution at 35 ºC from triplicate experiments.
80x41mm (300 x 300 DPI)

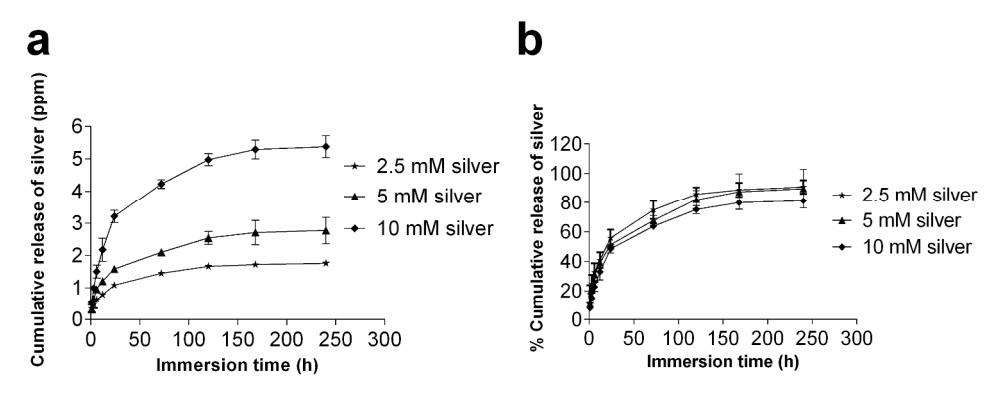

Figure 6. The cumulative release of silver from silver hydrogels after immersion in simulated body fluid solution at 35 ºC from triplicate experiments. a: cumulative release of silver (ppm), b: % cumulative release of silver.
276x111mm (300 x 300 DPI)

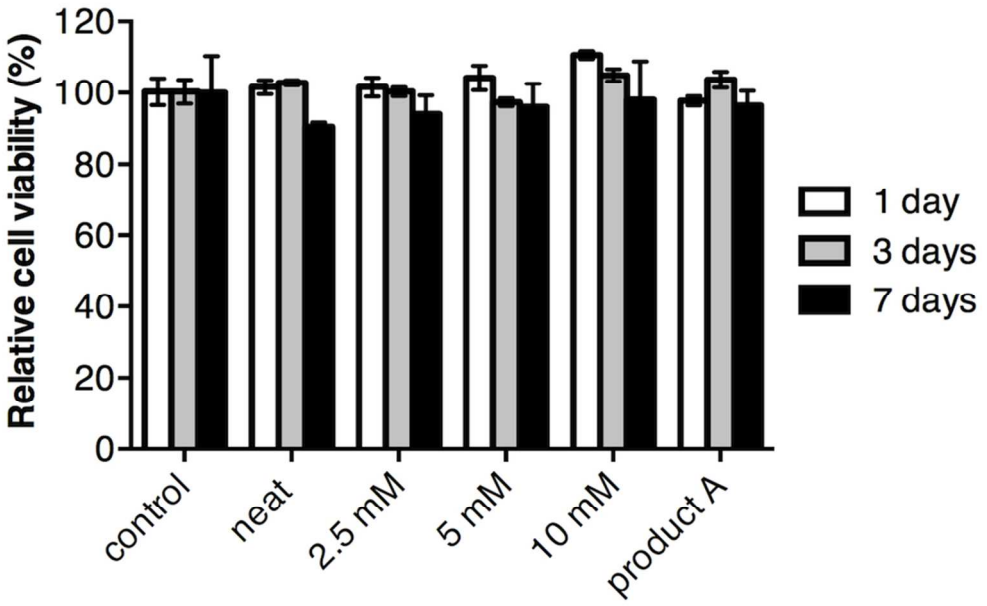

Figure 7. The cytotoxicity of the neat hydrogel, nanosilver hydrogels and product A on Normal Human Dermal Fibroblast cells from triplicate experiments.
80x50mm (300 x 300 DPI)

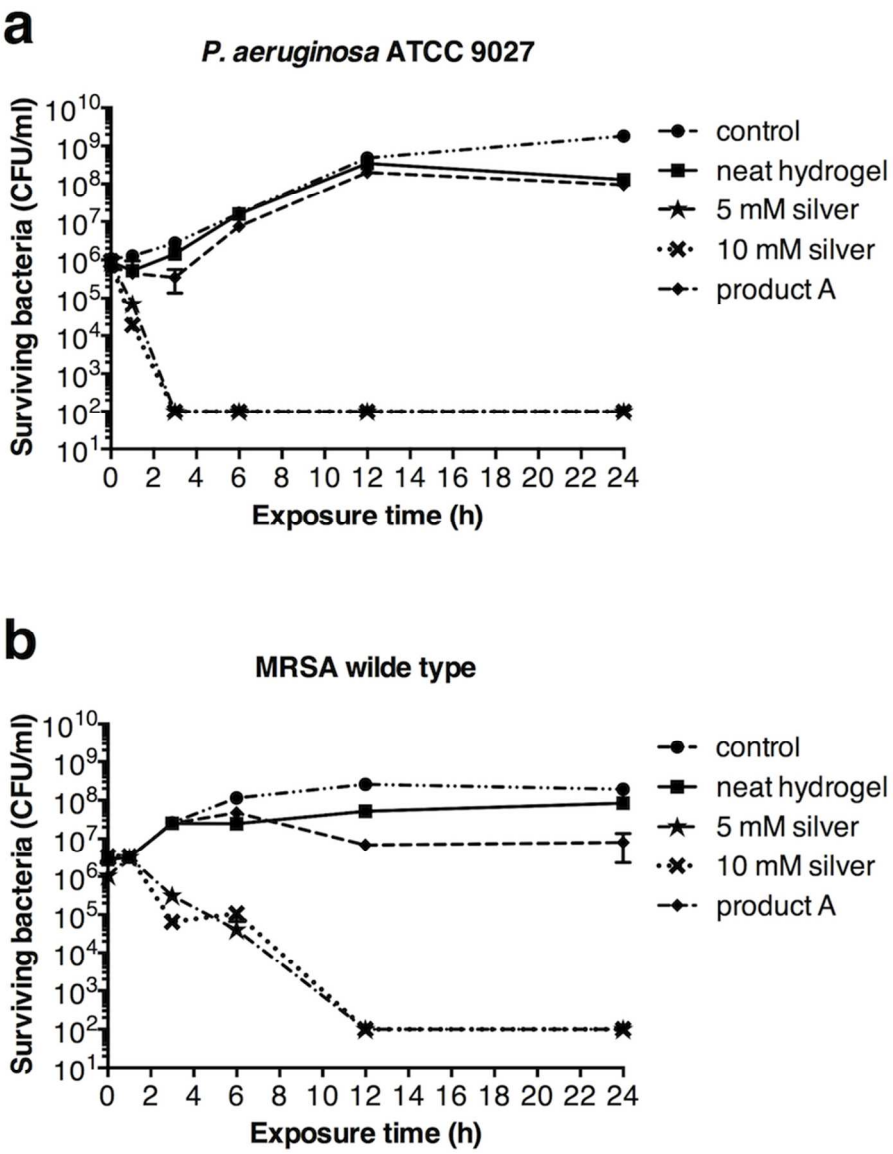

Figure 8. Bacterial survival curves of a: P. aeruginosa and b: MRSA exposed to neat hydrogel, silver hydrogels and product A from duplicate experiments.
80x102mm (300 x 300 DPI)

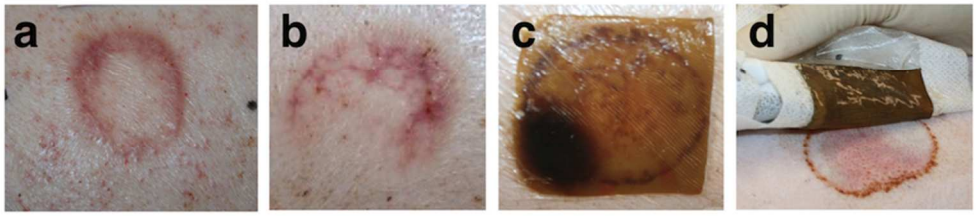

Figure 9. Photographs of a: control wound, b: wound treated with 5 mM silver hydrogel, c: the wound seen through the transparent 5 mM silver hydrogel, d: the 5 mM silver hydrogel after being removed from a wound.
80x18mm (300 x 300 DPI)

Figure 1. A schematic representation of polymerization of AMPS monomer with gamma irradiation. Silver ions were reduced to form SNP which were infused in the crosslinked polymeric network

Figure 2. The appearance of the radiated hydrogel pads darkened with increasing silver concentration. **a**: neat hydrogel, **b**: 2.5 mM silver hydrogel, **c**: 5 mM silver hydrogel, **d**: 10 mM silver hydrogel.

Figure 3. SEM images of **a** neat hydrogel, **b**: 5 mM silver hydrogel and **c**: 10 mM silver hydrogel.

Figure 4. TEM images from immersion solutions of silver hydrogels and histograms of size distribution from the respective TEM images. **a**: 2.5 mM silver hydrogel, **b**: 5 mM silver hydrogel and **c**: 10 mM silver. **d**: TEM images of selected single crystals of SNP released from 5 mM silver hydrogel.

Figure 5. The swelling behaviors of the neat hydrogel, silver hydrogels and product A immersed in simulated body fluid solution at 35 ºC from triplicate experiments.

Figure 6. The cumulative release of silver from silver hydrogels after immersion in simulated body fluid solution at 35 ºC from triplicate experiments. **a**: cumulative release of silver (ppm), **b**: % cumulative release of silver.

Figure 7. The cytotoxicity of the neat hydrogel, nanosilver hydrogels and product A on Normal Human Dermal Fibroblast cells from triplicate experiments.

Figure 8. Bacterial survival curves of **a**: *P. aeruginosa* and **b**: MRSA exposed to neat hydrogel, silver hydrogels and product A from duplicate experiments.

Figure 9. Photographs of **a**: control wound, **b**: wound treated with 5 mM silver hydrogel, **c**: the wound seen through the transparent 5 mM silver hydrogel, **d**: the 5 mM silver hydrogel after being removed from a wound.